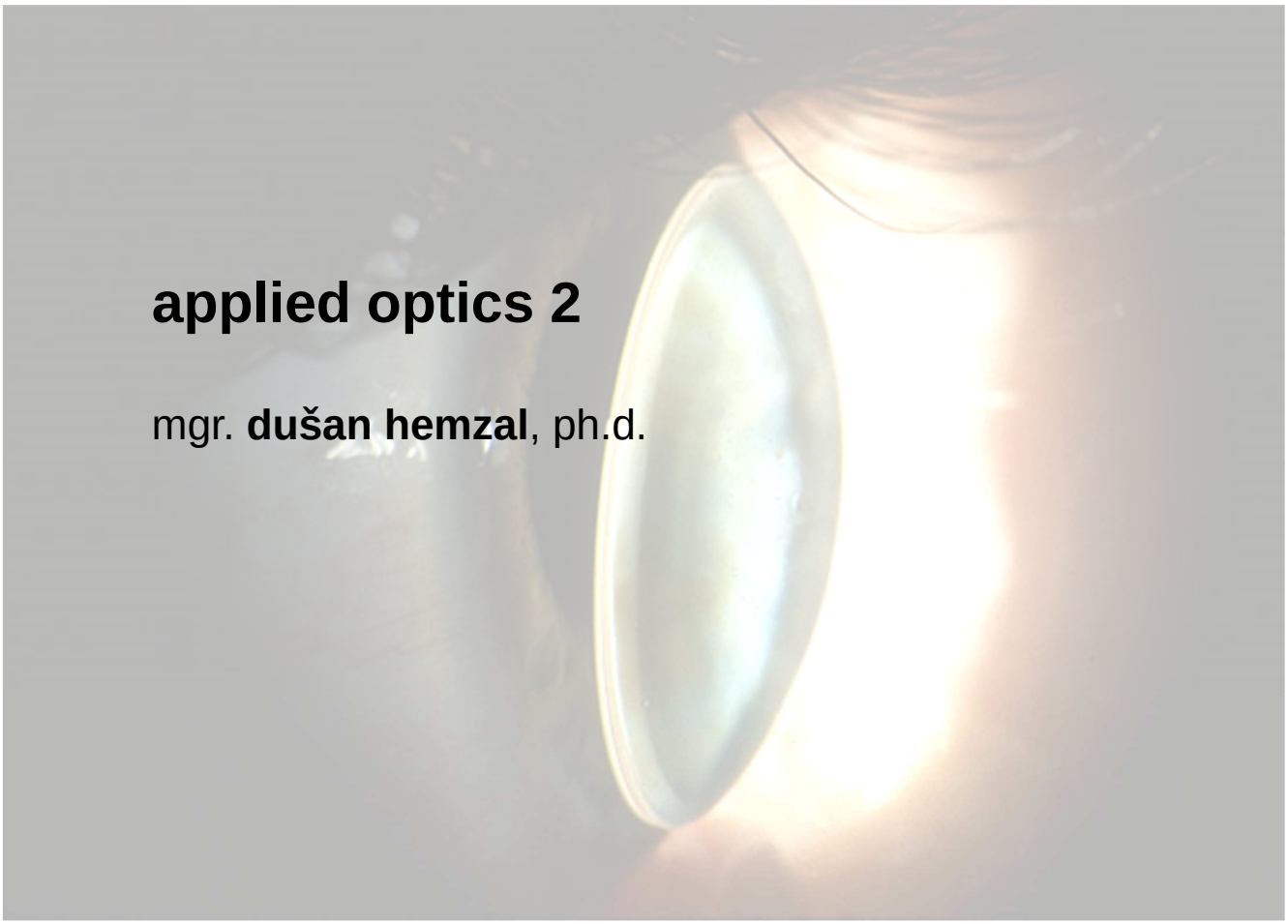

applied optics 2

mgr. **dušan hemzal**, ph.d.

applied optics 1:
properties of light

geometrical optics
polarisation and intensity of light
birefringence
interference
diffraction of light
scattering of light

applied optics 2:
application of light

sources and detectors of light
black body radiation, Bohr's model of atom, light bulb, discharge lamp, X-ray tube, lasers, H-D curve, CCD, *angiograph*

polarisation of light
polarisation microscope, *GDx*

interference and diffraction
biometry of the eye, *OCT*

wavefronts and aberrations
Seidel's aberrations, Zernike polynomials, wavefront error, classification of aberrations, *WASCA*

basic microscopy methods
bright field, dark field, Nomarsky contrast, immersion fluid, condensor, *endotellium microscope*

scanning methods
depth of field, confocal microscope, *HRT*, scanning techniques, *CSLO*

web: **http://www.physics.muni.cz/~hemzal/vyuka/optometry**

$$c = \lambda_0 f, \qquad \omega = 2\pi f, \qquad k = 2\pi n/\lambda_0$$

$$\delta = n_1 d_1 + n_2 d_2 + \ldots, \qquad \phi = \omega t - 2\pi\delta$$

$$\vec{k} = (k_x, k_y, k_z) := (0, 0, k_z)$$

$$\vec{E} = \begin{pmatrix} E_x \\ E_y \\ E_z \end{pmatrix} := \begin{pmatrix} E_{0x}(k) \cdot \cos(\omega t - k_z z + \phi_{0x}) \\ E_{0y}(k) \cdot \cos(\omega t - k_z z + \phi_{0y}) \\ 0 \end{pmatrix}$$

$$I = |\vec{E}_0|^2 = E_{0x}^2 + E_{0y}^2 \qquad \vec{E} \perp \vec{H} \perp \vec{k} \perp \vec{E}, \qquad \delta_c = \frac{\lambda^2}{\Delta\lambda}$$

$$I = I_1 + I_2 + 2\gamma\sqrt{I_1 I_2}\cos\Delta\phi, \qquad \mu = \frac{I_{\max} - I_{\min}}{I_{\max} + I_{\min}}$$

light sources

type of emission	**spectrum**
atomary emission	line/continuous
thermal emission	characteristic/contin.
luminiscence	~ monochromatic
Čerenkov radiation	continuous
annihilation	polychromatic

atomary emission, characteristic radiation — bremsstrahlung — Čerenkov radiation

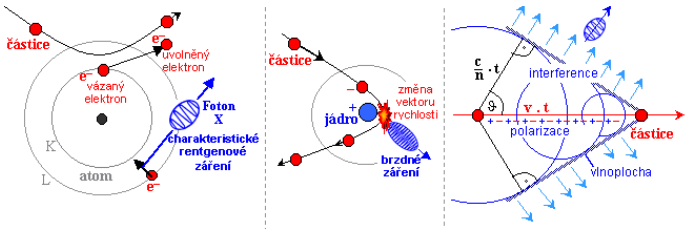

stimulated emission (lasers)

black body radiation

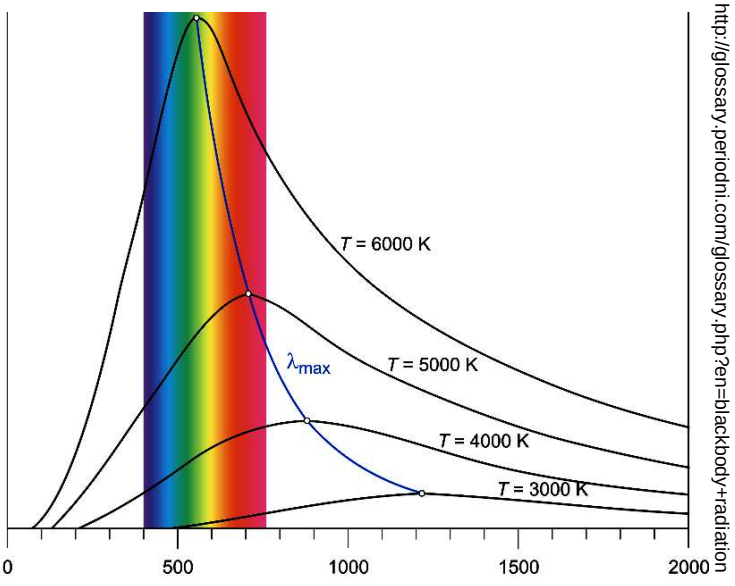

http://glossary.periodni.com/glossary.php?en=blackbody+radiation

maximum of radiated energy

$\lambda_{\max} = \frac{2{,}898\,mm}{T[K]}$ (Wien's law)

overall amount of radiated energy

$j \approx \sigma T^4$ (Stefan-Boltzmann law)

$\sigma = 5.67\text{x}10^{-8}\ \text{Js}^{-1}\text{m}^{-2}\text{K}^{-4}$

light bulb

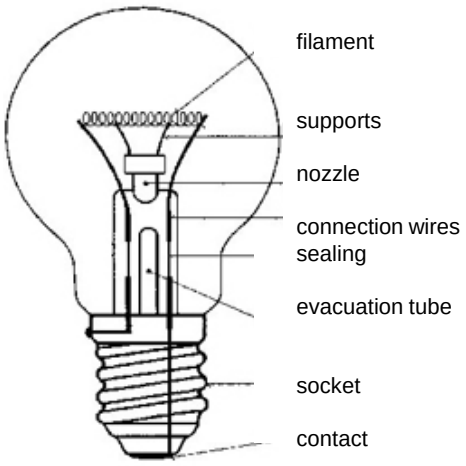

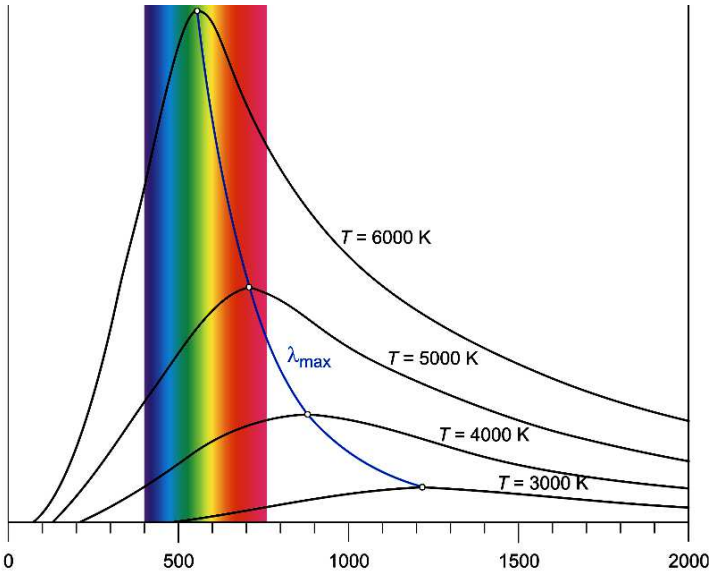

evacuated bulb with tungsten filament + nitrogen/argon atmosphere

electric current heats the filament to (2000 K – 3000 K)

cca 97% of energy is radiated in IR, only 3% in visible part of the spectrum

lifetime of bulb is limited by tungsten evaporation

for common use, light bulbs are being replaced (LED sources)

Bohr's model of atom

1 Å = 10^{-10} m = 0.1 nm

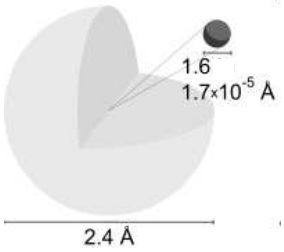

positive charge is concentrated in the nucleus, which occupies only a small fraction of atom volume (and is stabilized by presence of neutrons)

electrons orbit the nucleus using circular trajectories (or, at spherical shells)

the radii of the orbits are fixed if the atoms are to be stable
(radiative losses)

$$r_n = \frac{n^2\hbar^2}{k_e e^2 m_e Z} = \frac{n^2}{Z} a_0$$

where a_0=*0,522* Å is the **Bohr's radius**
(the radius of first shell in hydrogen)

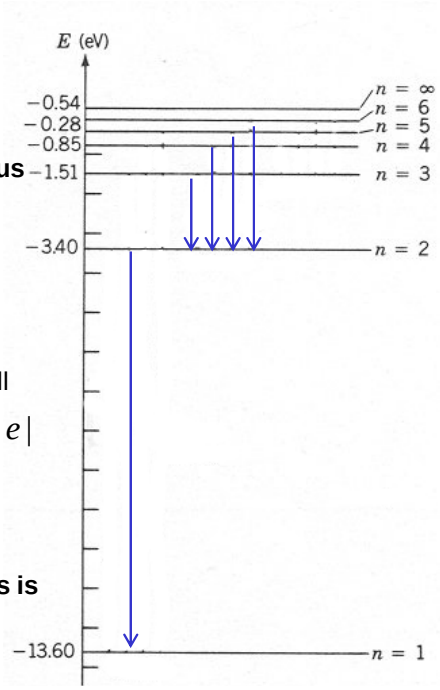

specific energy is prescribed to every orbit

$$E_n = -13.6\,\mathrm{eV}\,\frac{Z^2}{n^2}$$

-13,6 eV is the energy at first shell of hydrogen

$$E[\mathrm{eV}] = E[\mathrm{J}]/|e|$$

negative energies mean the electron is binded to the atom

the energy difference during electron transition between two orbitals is always accounted for by photon of appropriate wavelength
(emission or absorption, depending on the direction of transition)

X-ray tube

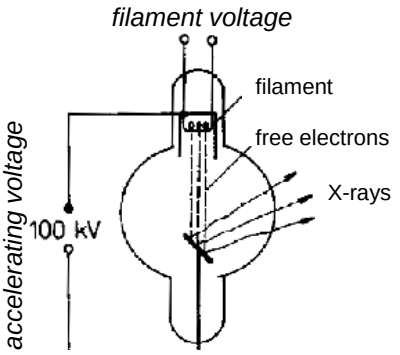

- evacuated tube with electrodes of special shape (filament cathode and disc anode)
- electric current heats the cathode up to creating free elecrons
- accelerating voltage directs the free leectrons toward the anode (impact speed of electrons at anode is more than 150 000 km/s at 100 kV)
- the heavier material of anode, the harder X-ray radiation is produced

during interaction of electrons with anode, two processes take place:

- **scattering** of X-ray light connected with the **bremsstrahlung**
- production of **characteristic radiation**, connected with **ejection of electrons** (close to the nucleus) and subsequent refilling of the gaps

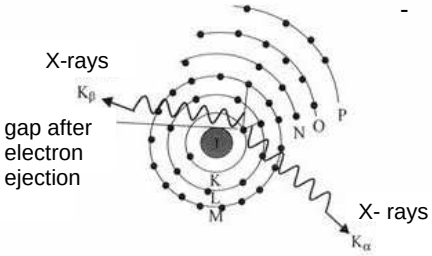

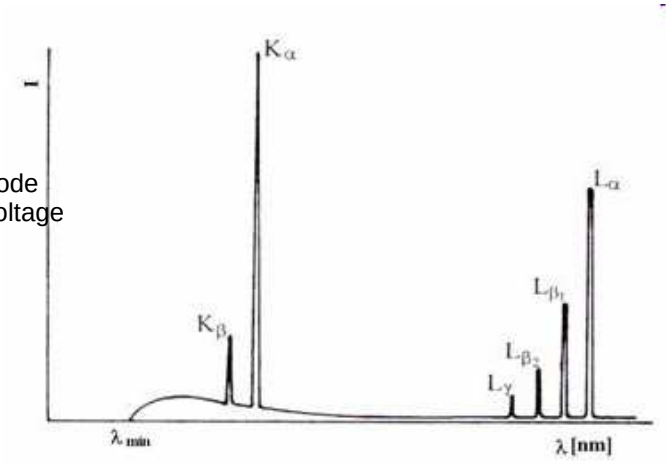

characteristic radiation: depends on the material of anode
independent of accelerating voltage

bremsstrahlung: independent of anode material
depends on accelerating voltage

breaking radiation cutoff:

$$\lambda_{\min} = \frac{hc}{e \cdot V}$$ (Duane–Hunt law)

stimulated emission – lasers

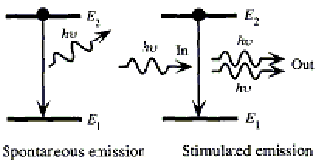

usually, excited states lifetimes are very short (about 1 ns), but occasionally, excited states are **meta-stable** (lifetimes about 1000 ns)

with sufficient **optical pumping**, electrons can be mustered at the meta-stable level
inversion of state: occupation of excited state is higher than that of base state
after random spontaneous emission, electrons exhibit chain de-excitaion via **stimulated emission** as perfect copies of the original photon

length of **resonator** selects the allowed wavelength of photons: $L = m\frac{\lambda}{2}$

as well as (together with mirrors used) the spectral line-width: $\Delta\lambda = \frac{\lambda_0^2(1-R)}{4\pi L\sqrt{R}}$

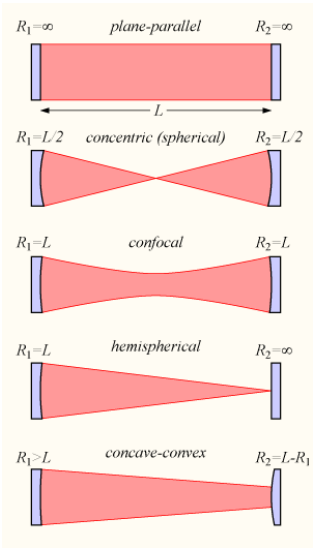

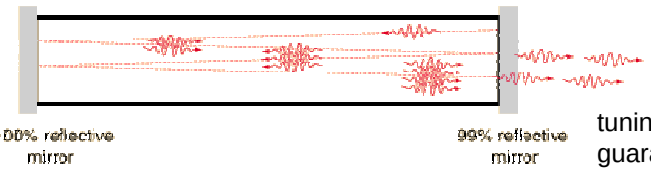

tuning of the mirrors guarantees **collimated** laser beam

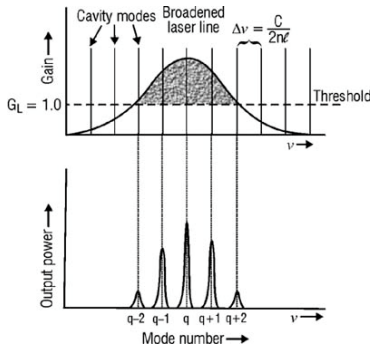

by combination of meta-stable transition spectral width and resonator modes width extremely narrow linewidth of laser is produced

using suitable mirror coating, only the central mode can be selected – laser becomes super **coherent**

apart from stimulation, laser uses a common type atomic emission

He-Ne laser

wavelength 632,8 nm, continual,
laser power up to 50 mW

a mixture of helium and neon in evacuated tube

pumping is realised by starting a discharge
in the tube

pumping excites mostly helium, the energy is
passed to neon (meta-stable levels) by collisions

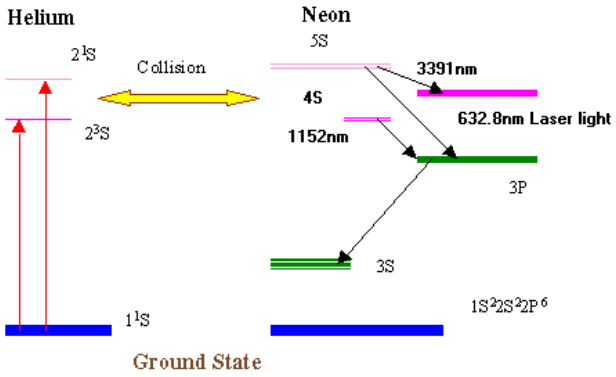

laser	*pumping*	*regime*	*application*
He-Ne (N - CO_2)	optical (discharge)	continual, 632,8 nm (continual, 1060 nm)	basic type laser
ruby laser: Al_2O_3 – Cr	optické (ionisation)	pulsed, 694,3 nm	tattoo removal
ion lasers : argon (krypton)	optical (discharge)	continual, 488 nm, 514 nm continual, VIS	coagulation (retina)
Nd:YAG	optical	pulsed, 1064 nm	iridotomy
excimer lasers.: ArF KrF (XeF,…)	chemical reaction	pulsed, 193 nm pulsed, 248 nm (353 nm)	ablation, LASIK
dye lasers: rhodamine 6G, stilbene	by another laser	pulsed, 570-640 nm pulsed, 390-435 nm	tunable lasers removal of moles

gas discharge

discharge lamp: evacuated tube with electrodes, secondarily filled with gas
upon **ionization**, a permanent discharge can be ignited in gas

- ionisation by voltage: glow discharge (ionisation by accelerated electrons)
- thermal ionisation: (spark) discharge

after ignition, discharges tend to be self-sustaining

low-pressure (**neon) tube** (tenths of kPa) with separate electrodes
color depends on gas composition (99.5 % neon, 0.5 % argon)
starting voltage about 120 V

with DC, only one electrode glows
with AC, both electrodes glow (as voltage changes sign)
power consumption is small

high intensity discharge

ignited by touching of the electrodes and their
subsequent withdrawal

can be produced in various atmospheres

problem: high current between electrodes make them
burn away (anode 4x faster than cathode)

most of the light come from heated electrodes
(anode 90%, cathode 8%, discharge itself 2%)

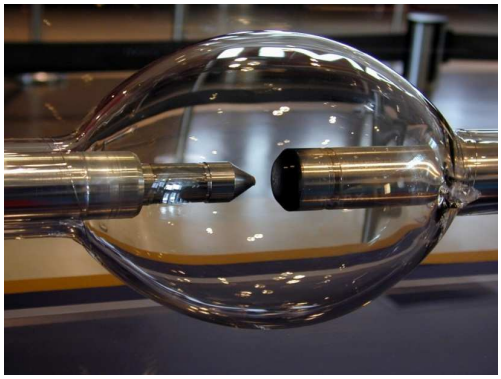

luminiscence

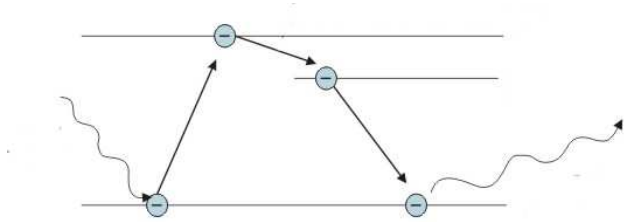

luminiscence is a common designation for light emission following some light absorption meanwhile non-radiative de-excitation also takes place

luminescent response is delayed from absorption, for longer delays we use the term phosphorescence

Stokes law: luminescence emission always takes place at wavelength higher than that of the absorbed light

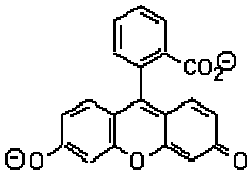

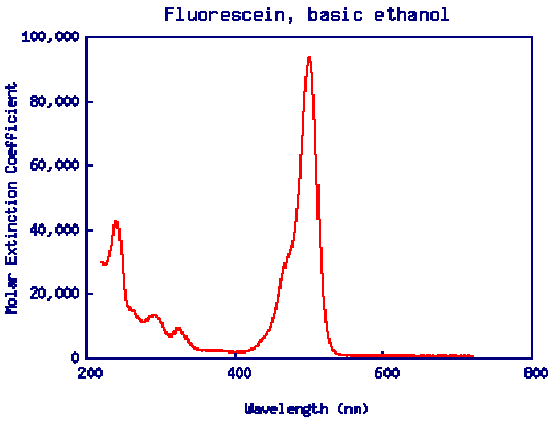

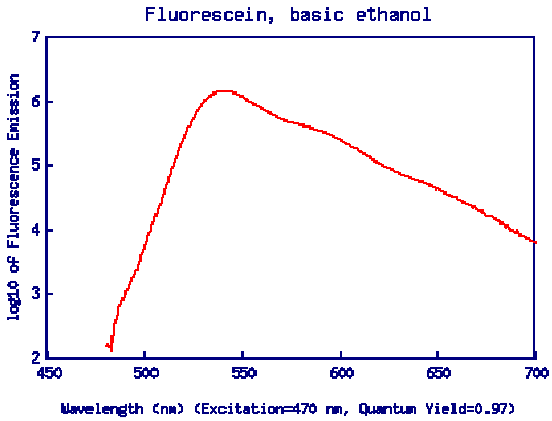

within 24 hours of fluorescein application, irradiation by green lasers (Ar-ion) is avoided

fundus camera and fluorescein angiography

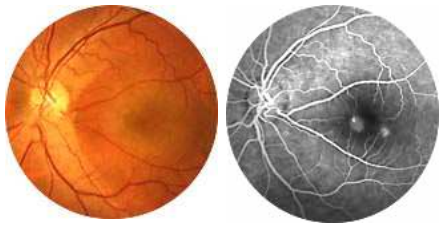

fluorescence: emissive response of material to illumination
delayed by miliseconds
red-shifted w.r.t. excitation

for longer delays (seconds or even more) we use term ph**osphorescence**

some tissues act as natural fluorophores, short illumination then suffices to trigger the response

or, artificial fluorophore can be supplied intravenously, eg

fluorescein absorbs in blue part of the spectrum (485-500 nm) and
emits in green part of the spectrum (525-530 nm)

indocyanine green (ICG) has absorbtion maximum near 800 nm and
emits light near835 nm (ie. whole phenomenon takes place in IR)

illumination of retina can be achived using the **fundus camera**

- special microscope serves as objective
- strong source of flash light is needed

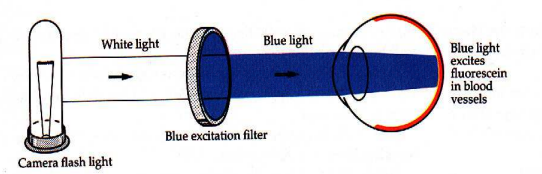

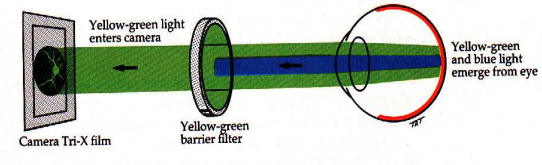

it is convenient to perform both measurements simultaneously

detection of light

the eye

response time 0,1s
detection via electrochemical chain

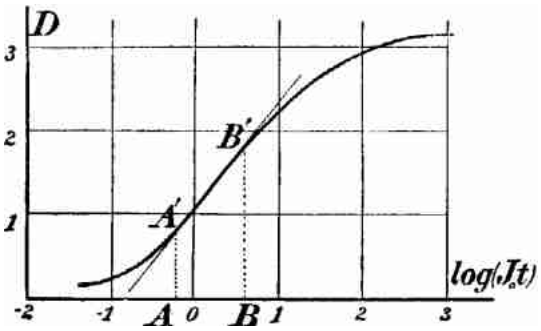

photographic emulsion

- **photosensitive layer** of halogenides of silver (eg. AgBr)
- in reaction to illumination, the silver is reduced (latent image is produced – amount of reduced silver too small to be visible)
- role of the **developer** (eg. $Na_2S_2O_3.5H_2O$) is to seek the places where silver has already been reduced and there multiply the amount of reduced silver (about billion times)
- the fixer changes the remaining AgBr into water soluble salt, which is subsequently washed away (together with gelatine matrix supporting the photosensitive layer)

- developing of the film must be stopped in due time
the response both to illumination and to developing is described by the general **Hurter-Driffield** curve

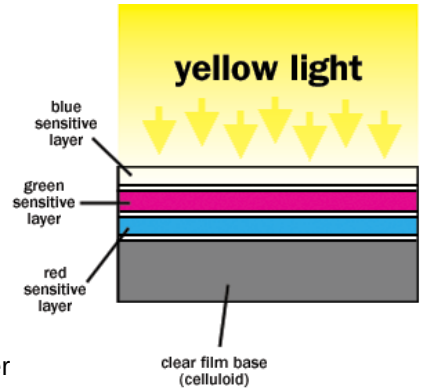

photographic emulsion works also with X-ray

insensibilised films are almost insensitive to green light
sensibilisation: ortochromatic, panchromatic

coloured film: three suitably sensibilised layers atop one another

detection of light

sensitivity of detectors can be measured as *s*[ASA]; for a correct exposition time *t*[s] of the observed scene the exposition need [EV] is introduced through

$$2^{EV_S} = \frac{c^2}{t}$$

where *c* is the speed of the objective used.
clearly, shift of exposition need by 1EV changes exposition time by factor of 2 (with *c* fixed)

exposition need of usual scenes is known (or can be measured), it is convenient to refer the value to a fixed detector sensitivity (say, 100ASA); for other speeds, one has

$$2^{EV_S - EV_{100}} = \frac{s}{100}$$

by combination of the two formulas one finally has

$$t = \frac{c^2}{\frac{s}{100} 2^{EV_{100}}}$$

common scenes range from EV_{100} = 16 (sunlit snow)
to EV_{100} = -9 (Milky Way).

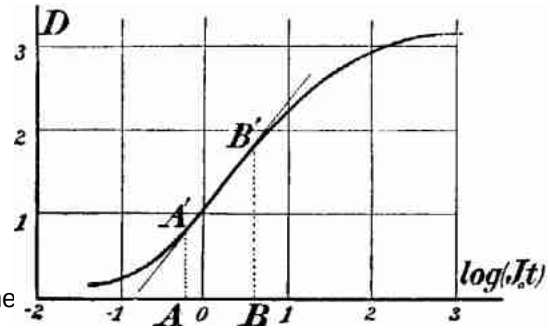

apart from exposition need, every scene also posses some **exposition extent** [ASA] describing the fluctuation of the forme within the scene:

dynamic range of the detector
exposition extent of the scene
exposition flexibility of the detector for the given scene

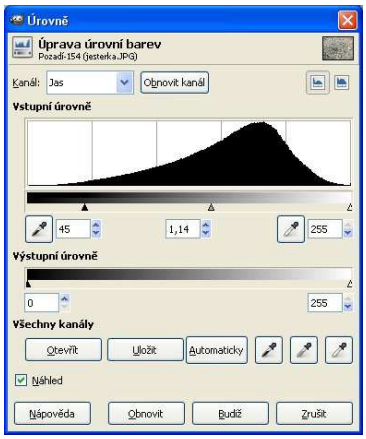

dark tones in image are missing
the image contrast is lowered

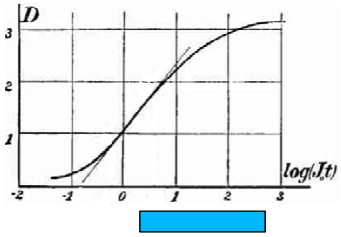

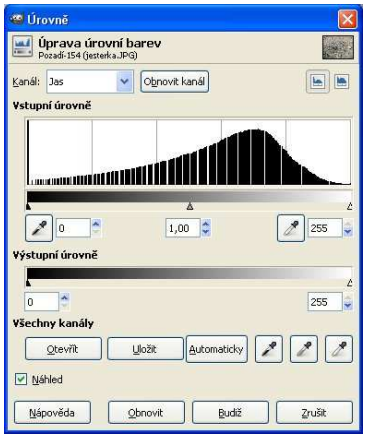

software repair is possible (to some extent)
contrast is improved, but colors get (slightly) unnatural

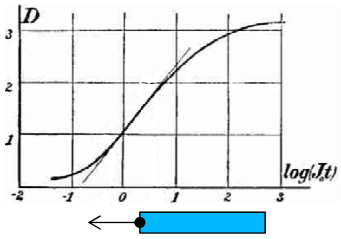

detection of light

CCD (Charge Coupled Device)

uses photoefect, descendant of a photodiode:
impacting light produces free electrons, that can be counted to provide relative measure of light intensity

condition for photon capture: $hf > A$

the work function ***A*** is a constant of each material, usually tenths to units of eV

technically, a CCD detector is realized by a MOS type semiconductor organized into distinct electrodes

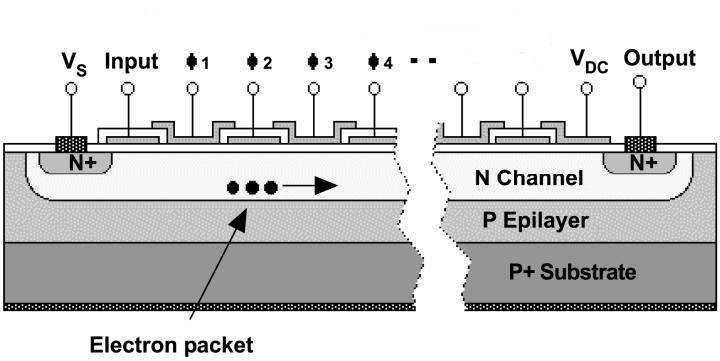

by suitable voltage gating the freed electrons can be held below the electrode
after exposition, clocking of the voltage shifts the pixels towards read out

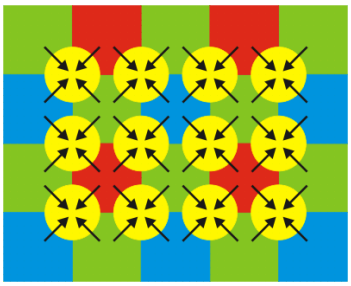

to achieve colored image, RGB masking is used (which decreases resolution of the chip)

photographic objective

focal length f

diameter of aperture D

objective speed $c = f / D$

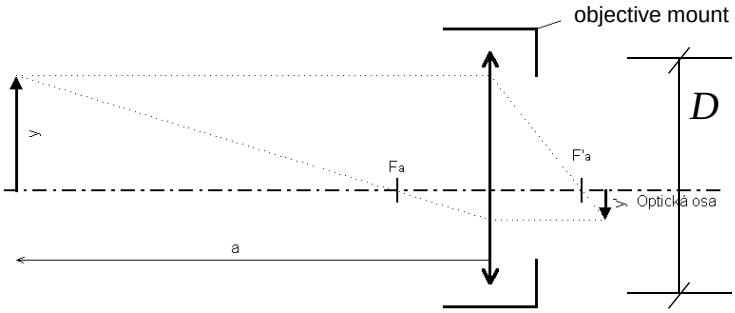

the distance of objective from detector selects which objects will be sharply imaged

from imaging equation: the farthest object are focused closest to the objective
as the objective mount is limited in travel, there exists
the closest focusable point (a_{min})

macro regime: by shifting of inner lenses within objective,
objects closer than a_{min} can be focused

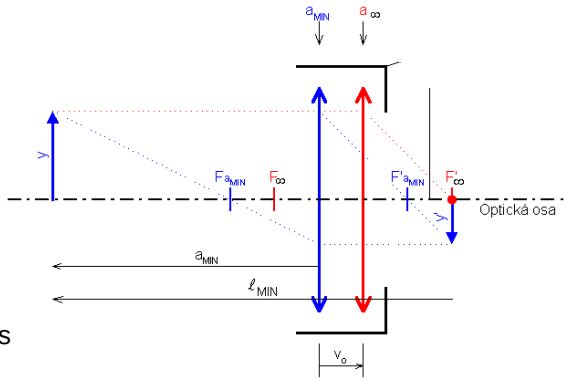

another solution: secondary lens

the size o of image of a distant point can be estimated as

$o \doteq f \tan \xi$ where ξ is the angle, under which we observe the object

depth of field

a perfect optical system images a point object into a point image
in the vicinity of this point image the rays form a cone, whose angle depends on the aperture

in real optical system the image is hampered at least by diffraction
the original cone with sharp tip at the image is replaced by a **diffraction tunnel**
whose waist opens only slowly and is surrounded by diffraction minima and maxima

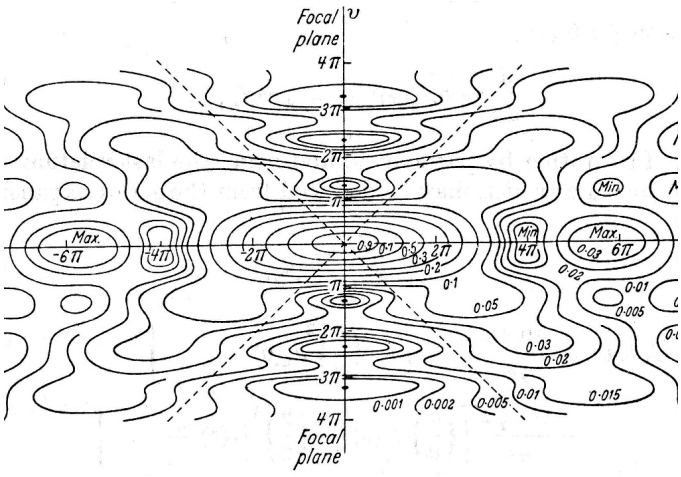

length of the diffraction tunnel:

$$\frac{l}{\lambda} = 4\frac{f^2}{D^2} = 4c^2$$

diffraction tunnel **waist** :

$$\frac{d}{\lambda} = \frac{3.8317}{\pi}\frac{f}{D} = \frac{3.8317}{\pi}c$$

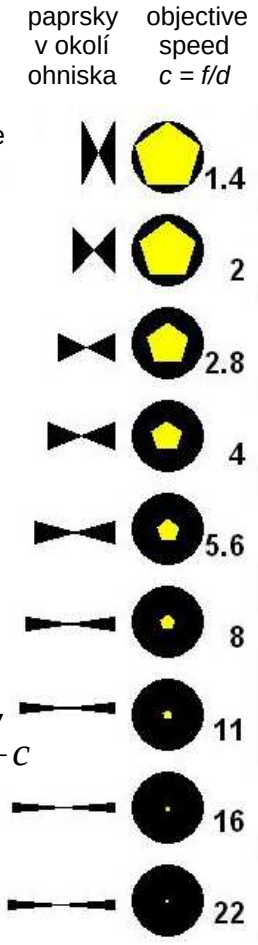

confocal microscope

patented 1957

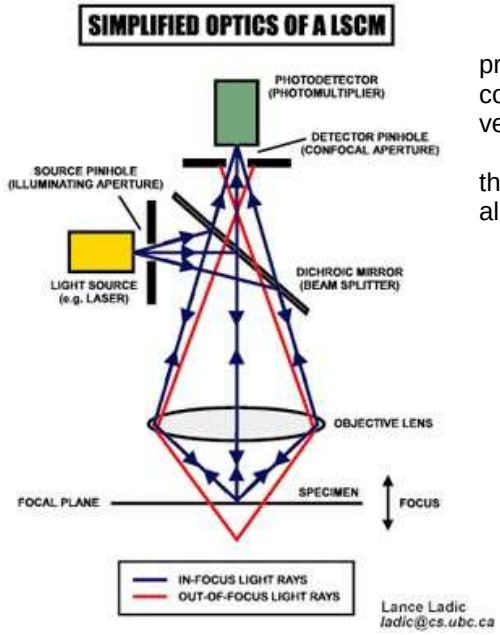

principle of the method: an aperture iris is introduced into the conjugate focus to the observed point. The opening of the iris is very small, and thus strongly limiting rays from other points.

the iris is (piezo) moved, so in result, a full 3D image can be taken albeit point by point, which is slow

usually, fluorescent image is taken

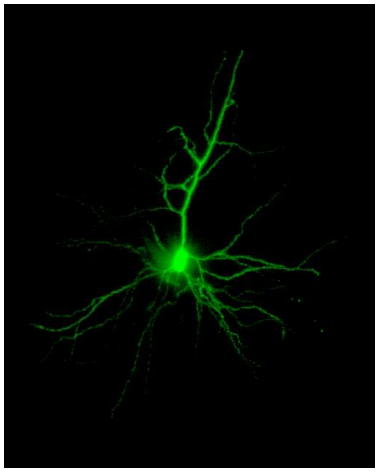

the image is processed by a computer

as the image is taken point by point, confocal microscope generally belongs to the class of scanning microscopes

Heidelberg Retina Tomograph (**HRT II, III**), 2005

confocal microscope setup, that
enhances the fundus camera possibilities
is suitable for glaucoma diagnosis

provides objective information
allows for progression monitoring

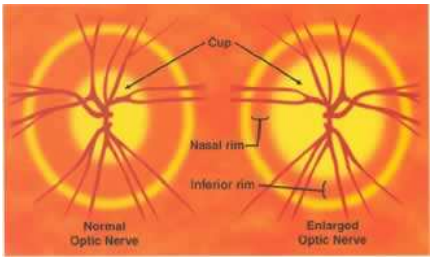

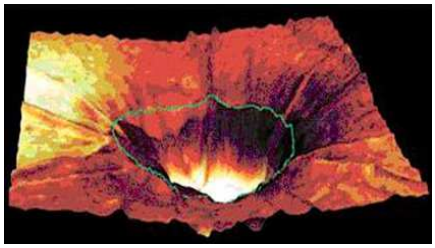

semiconductor laser, 670 nm
field of vies 15°x15°, centred to papilla of optical nerve

scans 384x384 points
16-64 layers of depth

triple repeat (statistics)

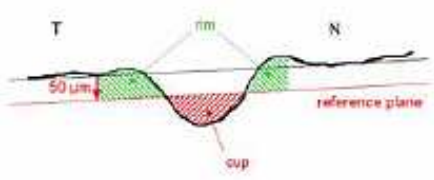

3D image is computed automatically
optic disc is segmented manually by an ophthalmologist

consequently, the computer calculates the relevant characteristics (usually in six angular segments):
size and shape of disc and cup, thickness of retinal layer, excavation

data can be checked again database, important is also a comparison of left/right eye

measurement can be performed through glasses/contact lenses, dilatation of pupil is not necessary

scanning microscopy techniques

when imaging large areas, it is convenient to take several subpictures which are aligned to final image

the aberration are easier to treat for smaller fields of view, but higher mechanical stability is required

scanning optics:

mechanical (slow): Nipkow disc, piesoelectrics

optical (faster, without mechanical vibrations):

Kerr cell, Pokelson cell, ultrasound bending of light

for fast detection, CCD is almost exclusively used

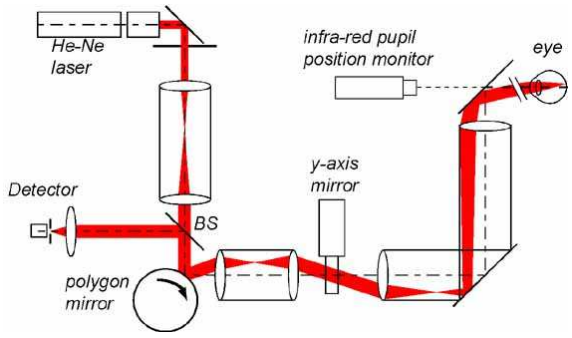

confocal scanning laser ophthalmoscope (CSLO) 1979

objective is the eye itself

allows imaging of individual photo-receptors at retina

images about 1,5° of retina with 30 scans/second

utilisation of adaptive optics allows to eliminate the aberrations of the eye (and distinguish the types of receptors)

used for direct observing of scotoms and retinal faults

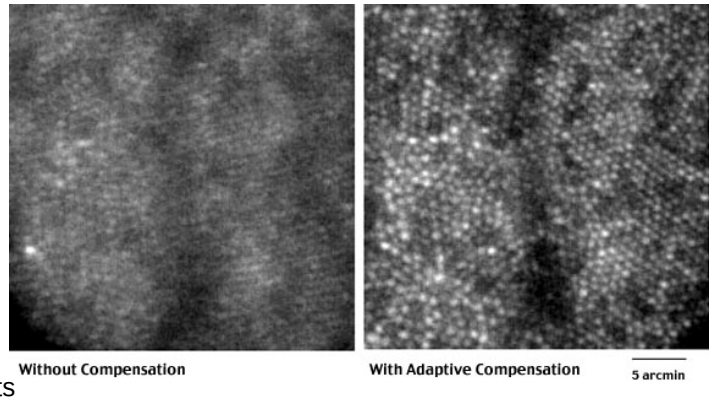

analysis of retinal neural layer thickness - GDx

the neural fibres are naturally birefringent (thanks to prolonged molecules in their shields)

for polarization microscopy, optical axes must be perpendicular to the line of sight – just the case of fibres at retina

as the light needs to be reflected (passing the neural layer forth and back), usually polarizer serves also as (parallel) analyser

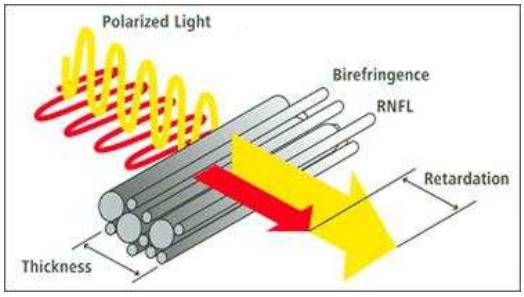

after polariser $E_p = E_x \cos(\omega t - kz)$

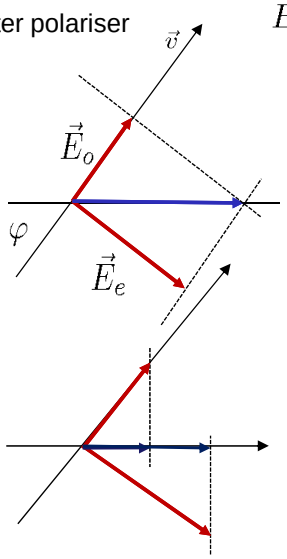

1) after entering the birefringent fibre

$$E_{||} = E_p \cos\varphi = E_x \cos\varphi \cos(\omega t - kz)$$

$$E_{\perp} = E_p \sin\varphi = E_x \sin\varphi \cos(\omega t - kz)$$

2) after reflection from fibre back-side

$$E_{||} = E_x \cos\varphi \cos(\omega t - kz - 2kn_o d)$$

$$E_{\perp} = E_x \sin\varphi \cos(\omega t - kz - 2kn_e d)$$

3) after analyser

$$E_{p||} = E_{||} \cos\varphi = E_x \cos^2\varphi \cos(\omega t - kz - 2kn_o d)$$

$$E_{p\perp} = E_{\perp} \sin\varphi = E_x \sin^2\varphi \cos(\omega t - kz - 2kn_e d)$$

both waves are now polarized in the same direction ad thanks to small thickness of fibres

ordinary and extra-ordinary rays remain coherent: interference takes place with phase shift $\delta = 2k(n_o - n_e)d$

analysis of retinal neural layer thickness - GDx

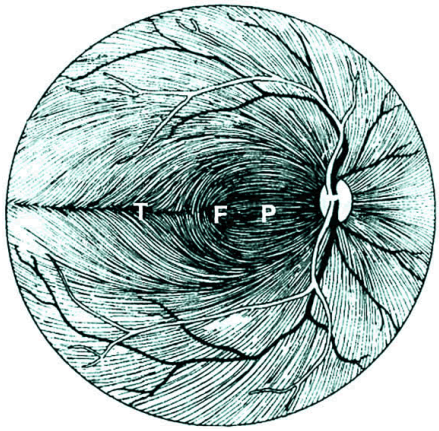

interference of two waves: $I = I_1 + I_2 + 2\sqrt{I_1 I_2}\cos\delta$

in our case

$$I = E_x^2\left(\cos^4\varphi + \sin^4\varphi + 2\cos^2\varphi\sin^2\varphi\cos\delta\right)$$

which can be written , using $E_x^2 = I_0$, also as

$$I/I_0 = 1 - \sin^2\frac{\delta}{2}\sin^2 2\varphi$$

for a particular fibre, $\delta = \text{konst}$, and thus rotation of polarizer produces minima and maxima of its visibility:

$$I_{\max}(\varphi = 0) = I_0 \quad I_{\min}(\varphi = \pi/4) = I_0\cos^2\frac{\delta}{2}$$

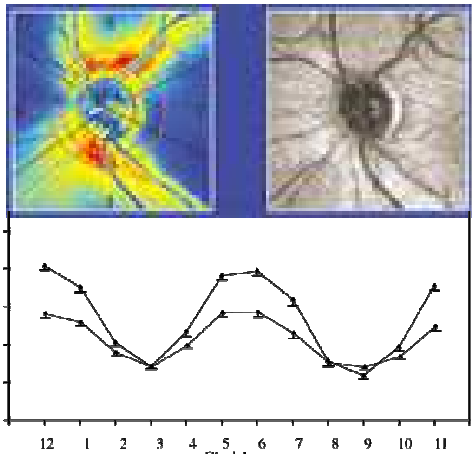

hence, the thickness of the fibre can de deduced from

$$\frac{I_{\max}}{I_{\min}} = \cos^2\frac{\delta}{2}$$

as the only unknown in $\delta = 2k(n_o - n_e)d$ is the thickness

the measurement of healthy tissue (top) and glaucoma affected one (bottom)

interference of light

for two monochromatic waves:

$$I = I_1 + I_2 + 2\gamma\sqrt{I_1 I_2}\cos\delta$$

visibility of the interference: $\mu = \dfrac{I_{\max} - I_{\min}}{I_{\max} + I_{\min}}$

coefficient γ measures the coherence $\gamma \in \langle 0, 1\rangle$ $I_1 \approx I_2 : \ \mu \approx \gamma$

Michelson interferometer

subtle shifting of one of the mirrors allows to measure sub-wavelength features by counting the passing fringes:

$$\Delta L_m = m\frac{\lambda}{2}$$

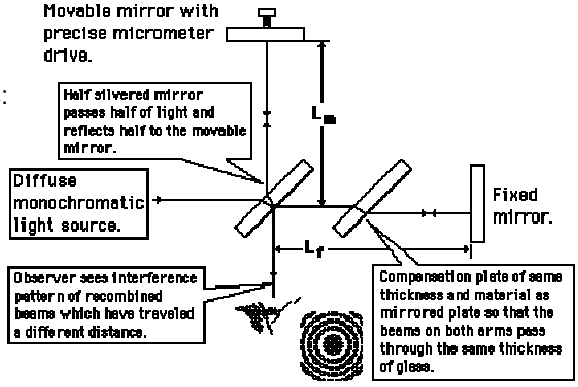

wave packets

$$E = \sum_{i=1}^{n} E_{0i}\cos(\omega_i t - k_i x + \delta_i)$$

the (coherence) length of the packet:

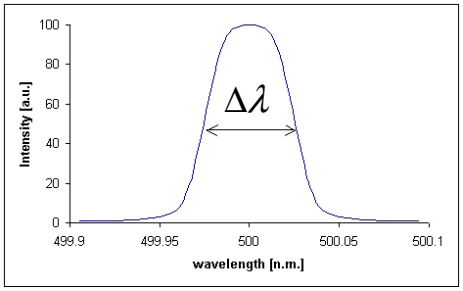

$$\delta_c = \frac{\lambda_0^2}{\Delta\lambda}$$

the packets will (partly) interfere, if they (partly) overlap in space

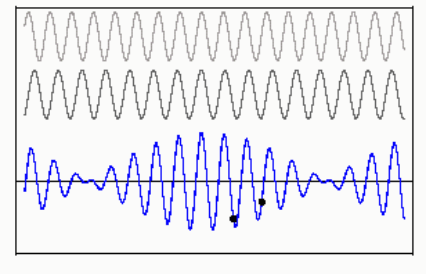

interferometric measurement of thickness

consider Michelson interferometer with moving mirror, sample of thickness *x* and refractive index *n*
we use the wave-packets picture:

the wave directly reflected packet (orange) and back-side reflected packet (green) will only interfere, when they succeed to meet both in space and time.
the phase difference in flight, caused by the sample thickness can be compensated by moving the interferometer arm
by scanning the full range of the arm movement, several peaks of interference visibility are observed, from which the thicknesses of individual layers within sample can be deduced

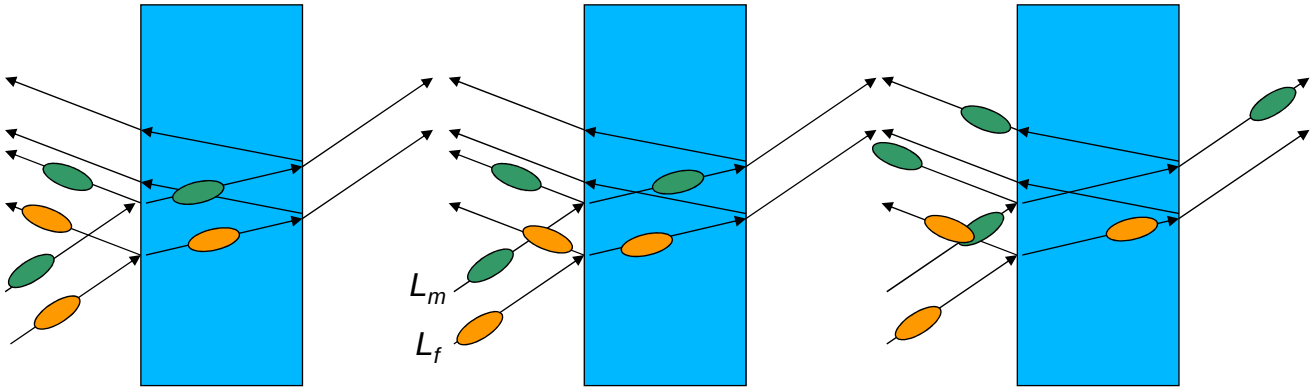

$\Delta d = 0$ $\Delta d \approx 0$ $\Delta d \approx 2nx$

higher order reflections are difficult to observe (their intensity is low)

optical biometry of the eye

IOL Master – performs interferometric measurement of structures within the eye using the wave-packets of suitable length

the method is non-contact: measurement can take place through glasses or, even through cataract

resolution in thickness: 0.02 mm

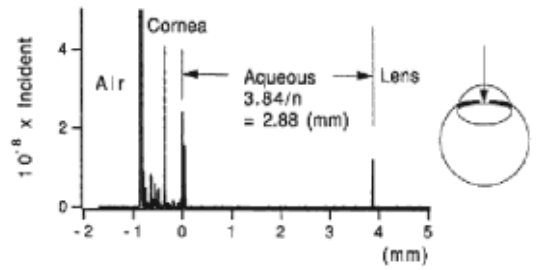

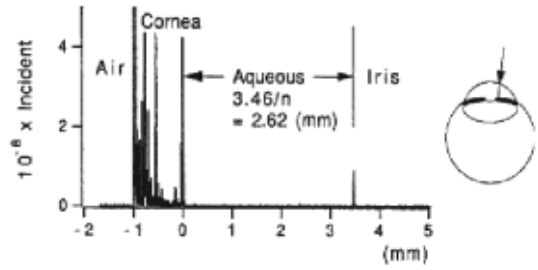

the output of measurement consists in dependence of interference visibility on the interferometer arms position

decomposition into possible reflecting surfaces is performed by a computer

the precision (stability) of the decomposition is highly improved (at sake of computational load) if multiple reflections can be taken into account

Optical Coherence Tomography (OCT), 1991

semiconductor laser diode, 800 – 1000 nm, hundreds of mW

the depth and lateral resolutions are detached:

depth resolution:
dependson packet length only $\ln(2)\frac{2}{\pi}\frac{\lambda_0^2}{\Delta\lambda}=\frac{2\ln 2}{\pi}\delta_c$

lateral resolution: depends on optics used

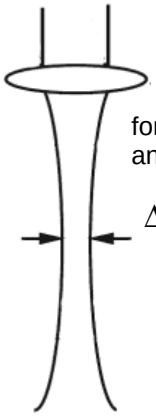

for an objective with focal length *f*
and numerical aperture *NA:*

$$\Delta x = 0.37\frac{\lambda_0}{NA}$$

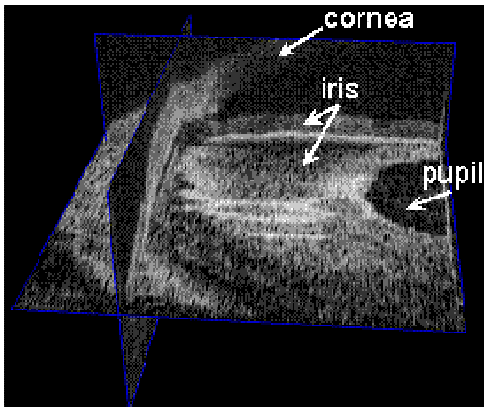

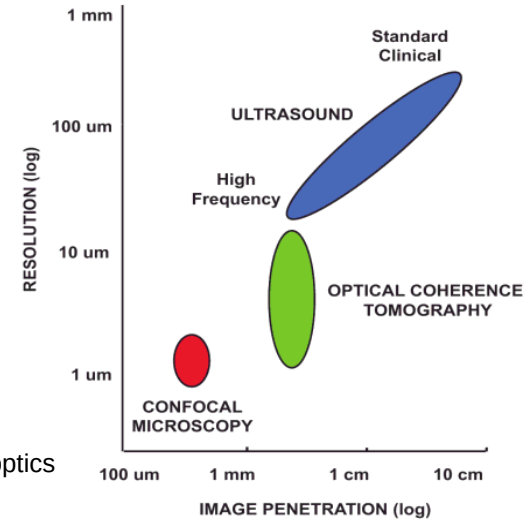

OCT = source of diffuse spectrum + interferometer + scanning optics

Optical Coherence Tomography (OCT), 1991

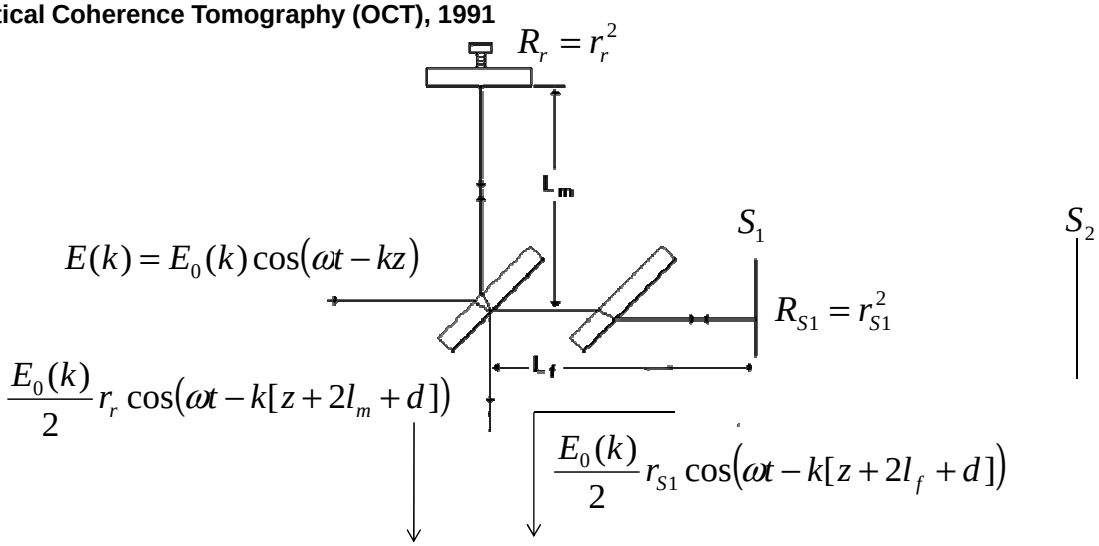

$$I = \frac{I_0(k)}{4}(R_r + R_{S1}) + 2I_0\sqrt{R_r R_{S1}}\cos(2k[l_f - l_m])$$

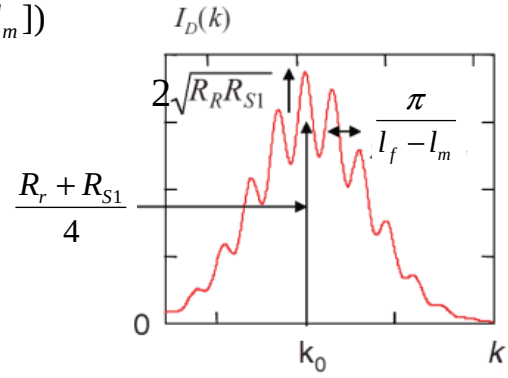

two successive maxima:

$$2k(l_f - l_m) = c2\pi$$

$$2k'(l_f - l_m) = (c+1)2\pi$$

$$\Delta k = k' - k = \frac{\pi}{l_f - l_m}$$

wavefront aberration in axially symmetric systems

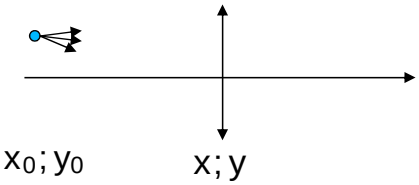

$\vec{x}_0 = (x_0, y_0)$ $\vec{x} = (x, y)$

without loss of generality, we can set $y_0 = 0$

based on the symmetry, rotating the system around the optical axis must produce no visible effect

only combinations of scalar products $\vec{x}_0 \cdot \vec{x}_0, \vec{x} \cdot \vec{x}_0, \vec{x} \cdot \vec{x}$ can be present

wavefront aberration: $H(x_0, y_0, x, y) \to H(x_0^2, x_0 x, x^2 + y^2)$ ($y_0 = 0$)

in polar coordinates $x = \rho \cos\vartheta$ $y = \rho \sin\vartheta$ ρ is the aperture radius

$$H(x_0^2, x_0\rho\cos\vartheta, \rho^2) = \sum_{k,l,m} W_{klm} x_0^k \rho^l \cos^m\vartheta =$$

$$= W_{000} + W_{200}x_0^2 + W_{111}x_0\rho\cos\theta + W_{002}\rho^2 +$$

$$+ W_{400}x_0^4 + W_{040}\rho^4 + W_{131}x_0\rho^3\cos\theta + W_{222}x_0^2\rho^2\cos^2\theta +$$

$$+ W_{220}x_0^2\rho^2 + W_{311}x_0^3\rho\cos\theta + \ldots$$

special case: axial (point) source: $x_0 = 0$

Seidel's aberrations 1856 (axially symmetric systems)

$$H = \frac{1}{8}S_I\rho^4 + \frac{1}{2}S_{II}x_0\rho^3\cos\vartheta + \frac{1}{2}S_{III}x_0^2\rho^2\cos^2\vartheta + \frac{1}{4}(S_{III} + S_{IV})x_0^2\rho^2 + \frac{1}{2}S_V x_0^3\rho\cos\vartheta$$

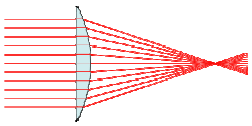

the lowest (third) order terms:

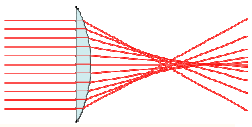

spherical aberration S_I, coma S_{II}, astigmatism S_{III}, curvature S_{IV}, distortion S_V

piston, tilt and defocus are not aberrations (they do not disturb point imaging)

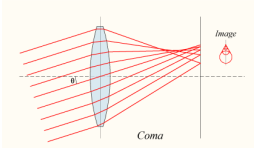

within higher orders, new types of aberrations are introduced (elliptic coma, …)

advantage of Seidel coefficients:

the overall aberration of every kind is just a sum of contributions from individual surfaces:

eg. $S_I = S_I^1 + S_I^2 + S_I^3 + S_I^4 + \ldots$ etc.

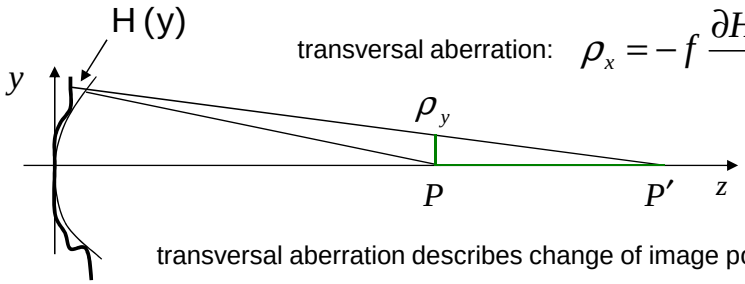

transversal aberration: $\rho_x = -f\frac{\partial H(x,y)}{\partial x}$ $\rho_y = -f\frac{\partial H(x,y)}{\partial y}$

transversal aberration describes change of image position within image plane

aberrations of human eye

motivation: information is needed in more detail than keratograph can provide

also, axial symmetry is nor present within eye
on the other hand, pupil is almost perfectly circular

Zernike polynomials (1934)

well suited for aberrations of the eye description, other systems (turbulent media, brilliant cutting) may be better described by other systems

we stat again from wavefront description using the polar coordinates $x = \rho\cos\theta, y = \rho\sin\theta$ in the plane of exit pupil:

$$H(\rho,\theta) = \sum_{n=1}^{k}\sum_{m=-n}^{n} W_n^m Z_n^m \qquad Z_n^m = R_n^m(\rho)\Phi_n^m(\theta)$$

drawback: information on position of the source is suppressed
for a complete aberrational description, several measurements are needed

advantage: individual terms do not interfere – addition of one polynomial does not disturb the other aberrations

one Zernike polynomial comprises several Seidel aberrations, and vice versa

individual Zernike polynomials and the wavefront errors produced:

axially symmetric aberrations are located on the axis of the triangle

'diamond' of Seidel aberrations stretches over several lines

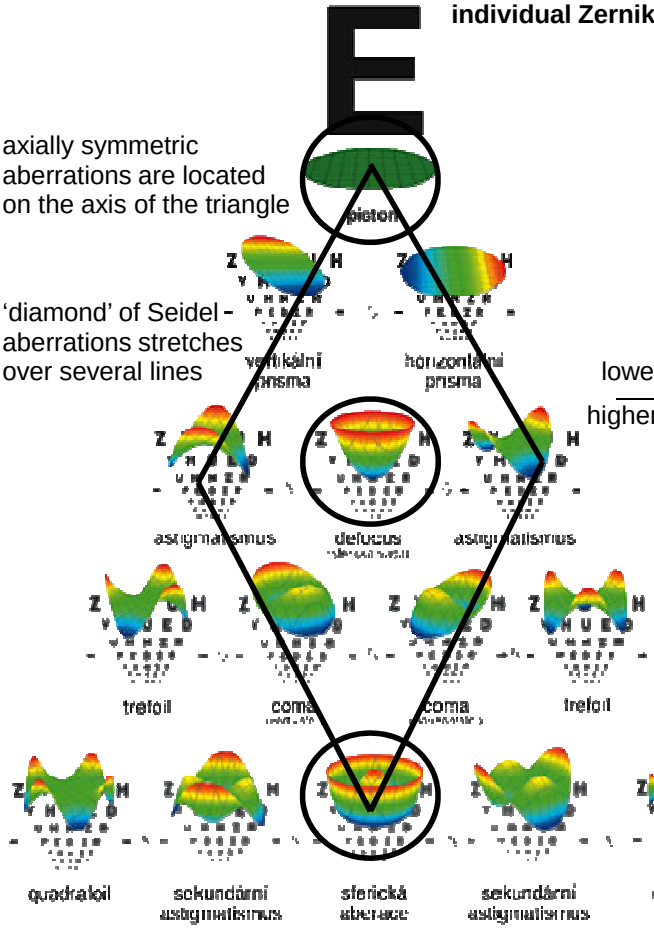

n	m	$Z_n^m(\rho,\theta)$
0	0	1
1	-1	$2\rho\sin(\theta)$
1	1	$2\rho\cos(\theta)$
2	-2	$\sqrt{6}\rho^2\sin(2\theta)$
2	0	$\sqrt{3}(2\rho^2-1)$
2	2	$\sqrt{6}\rho^2\cos(2\theta)$
3	-3	$\sqrt{8}\rho^3\sin(3\theta)$
3	-1	$\sqrt{8}(3\rho^3-2\rho)\sin(\theta)$
3	1	$\sqrt{8}(3\rho^3-2\rho)\cos(\theta)$
3	3	$\sqrt{8}\rho^3\cos(3\theta)$
4	-4	$\sqrt{10}\rho^4\sin(4\theta)$
4	-2	$\sqrt{10}(4\rho^4-3\rho^2)\sin(2\theta)$
4	0	$\sqrt{5}(6\rho^4-6\rho^2+1)$
4	2	$\sqrt{10}(4\rho^4-3\rho^2)\cos(2\theta)$
4	4	$\sqrt{10}\rho^4\cos(4\theta)$
⋮	⋮	⋮

lower aberrations

higher aberrations

Hartmann-Shack sensor

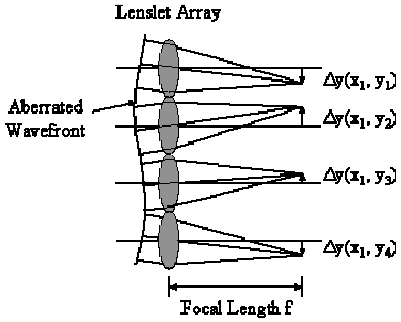

generalization of examination using single spherocylindrical lens

either two crossed rows of linear lamels,
or directly a 2D etched system of micro-lenses (*lenslet array*)

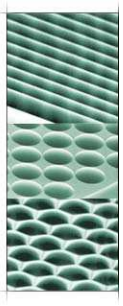

each lenslet focuses a small piece of wavefront
in this way, waveront aberrations is visualised through irregularity in the 2D grid of focused points
common parameters: 15-1000 μm/lens diameter,
accuracy of focus: +- 3%, substrate: (Si,Ge, ZnS) 1-6 mm thick

WASCA (WAve Aberration SCAnner)

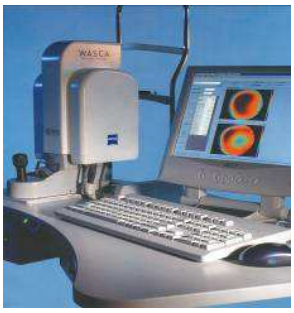

in combination with LASIK, aberrations up to 20th order can be corrected (not the case in practice – progression)

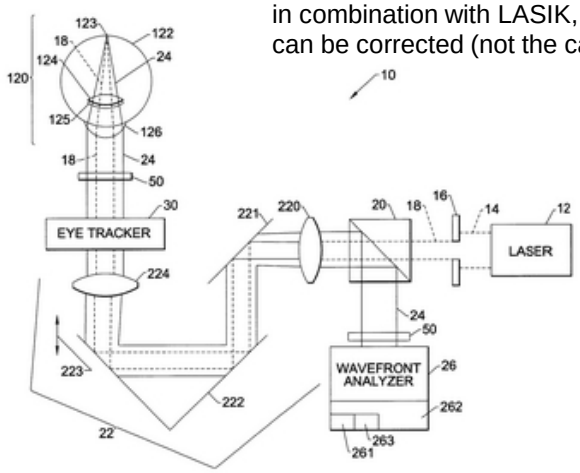

PSP (**P**oint **S**pread **F**unction):
shape of the real image of point source of light

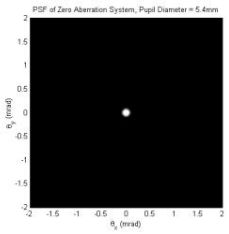

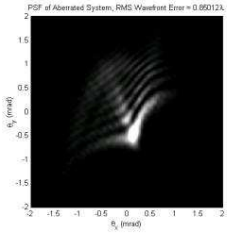

resolution limit of the objective

resolution of common detectors:
the eye (1 arc minute), photographic film (100 lines/mm), CCD (size of the pixel: 1-5 μm)

diffraction over circular aperture of radius R:

$$I \approx f^2(kR\rho / r_0)$$

first maximum (the Airy disc) contains about 80% of transmitted light

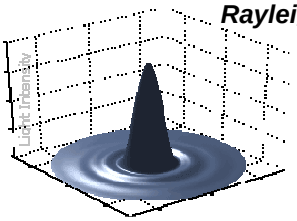

Rayleigh limit of resolution:

two point sources can be distinguished, if their images are at least the diameter of Airy's disc apart

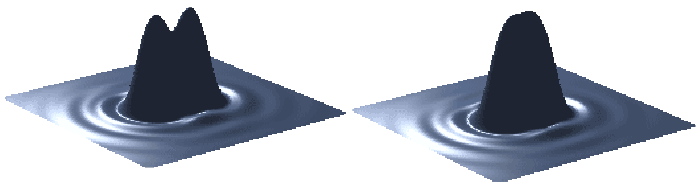

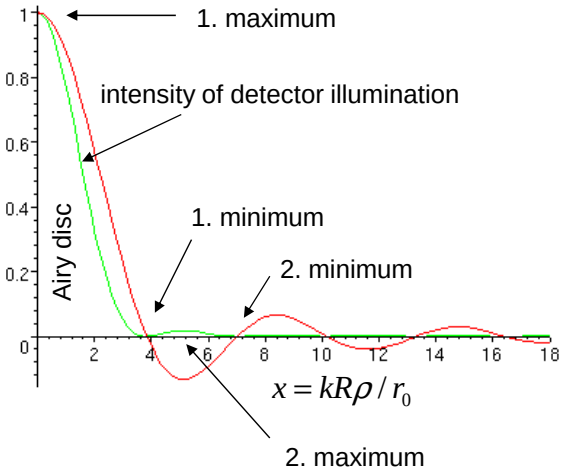

minima of intensity at the detector:
3.83, 7.02, 10.17, 13.32, 16.47…

in terms of angular separation: $\xi_k = \frac{144''}{D[\mathrm{mm}]}$

similar considerations hold for imaging of moving objects:
motional blur appears (blood flow etc.)

illumination of microscopy samples

light bulbs: wolfram filament
(halogen bulbs: wolfram filaments + iodine cycle)

discharge lamps: significant emission in UV
intense sources + good for luminescence trigering

filters: coloured - monochromatic, can improve image sharpness
gray (ND) - overall intensity tuning, can improve contrast

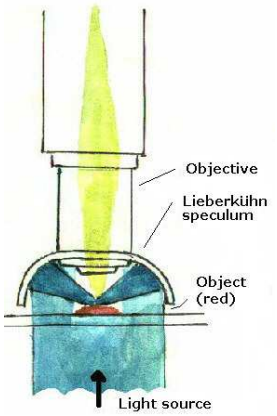

Lieberkuhn mirror

condenser serves to

homogenise light (intensity), creation of plane wavefront
increase the numerical aperture (and thus also the resolution of microscope)
allow for advanced microscopy techniques

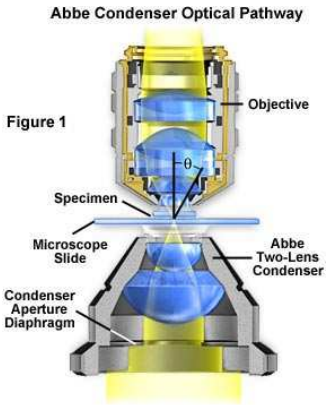

$$d_{\min} = \frac{\lambda_0}{A_0 + A_C} = C\frac{\lambda_0}{A_0} \qquad C \approx 0.5 \div 1$$

condensers can be constructed for both transmitted and reflected light
the advanced techniques are usually realised through filter wheels
condenser can be the most expensive part of the microscope

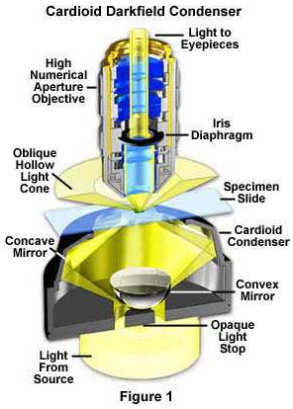

immersion objectives

through numerical aperture, the diffraction spot size depends on refractive index o the medium between objective and sample:

$$d_{\min} = \frac{1{,}22\lambda}{NA} = \frac{1{,}22\lambda}{n\sin\alpha}$$

one way of shifting the resolution limit is to use shorter wavelength light

the other is to introduce (immersion) medium with n>1 between objective and sample:

medium	n
air	1,0003
water	1,33
immersion oil	1,515
bromnaphtalene	1,658
metyleniodid	1,740

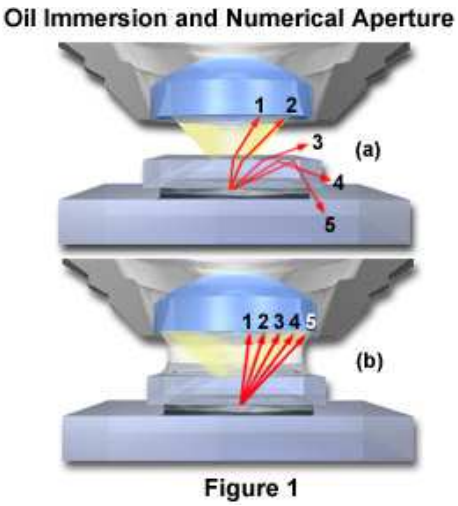

the resolution enhancement upon using immersion fluids comes from collecting higher angle rays

immersion objectives are explicitly prepared for contact with fluids (and are usually marked around by a colored line)

yet another possibility is to make use of condenser

(altogether, by application of all possible improvements, about a quarter of a wavelength can be resolved)

dark field (transmission and reflection)

bright filed: almost all light rays from source are used for creating an image; when no sample is present. homogeneously lit field (bright field) is observed

after sample loading, the viewed contrast is created by absorbing parts of the sample

samples with neglibigle absorption contrast get invisible using tis method

dark field: a hollow light beam is created within condenser, which reaches sample at an oblique angle, which is designed such, that these rays cannot be collected by the objective

hence, only light scattered by the sample can aid in constructing the image (scattering is omni-directional)

the hollow light beam is initiated using concave mirror similar construction can be reached in reflected light

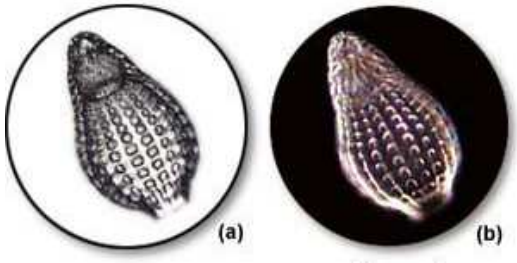

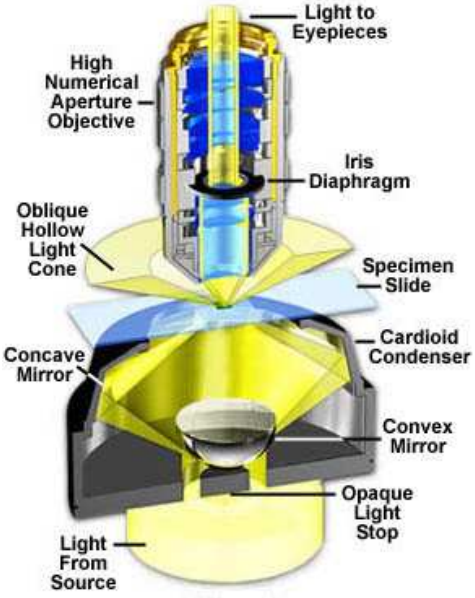

reminder: HRT also works in dark field

phase contrast (Zernike 1930, Nobel prize 1953)

samples, that exhibit both little absorption and little scattering will still be almost invisible
final solution: slight changes in refractive index need to be visualised

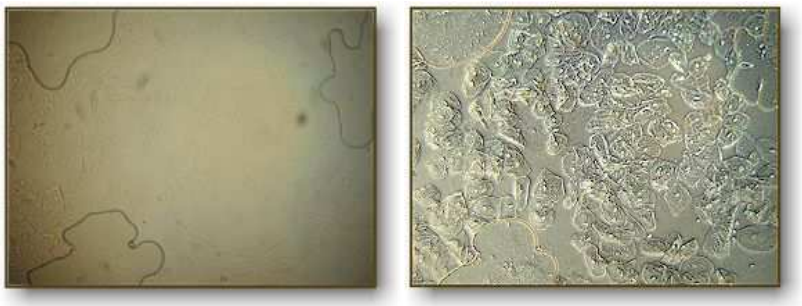

for biological samples, partial solution would be cell staining
but stained cells die

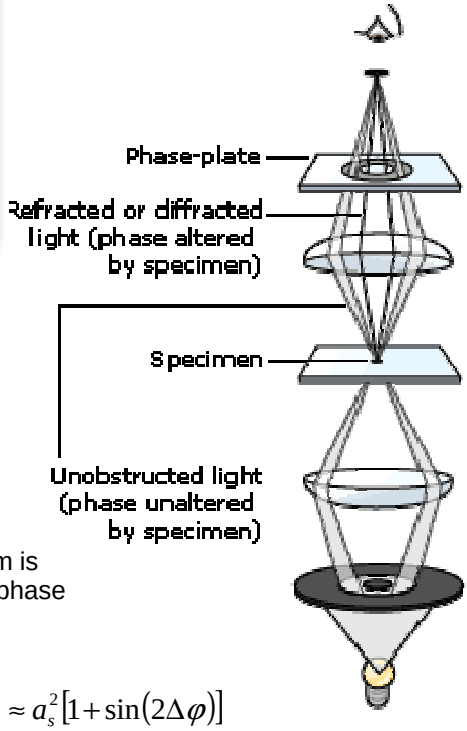

inhomogeneous refractive index causes both deviation and phase difference between any two originally close rays

the task of the microscope is to transfer the phase shift into intensity contrast

within condenser, ring with annular opening is placed – hollow light beam is created again, but this time, it is allowed to reach the objective (without phase shift)

after the sample, a secondary phase-plate is inserted which mixes the inner (phase modified) and outer light rays:

$$I'_s \approx a_s^2\left[1+\sin\left(2\Delta\varphi\right)\right]$$

DIC (differential interference contrast)

improvement of phase contrast modality: removal of the halo

especially useful for samples creating about λ/4 phase shift

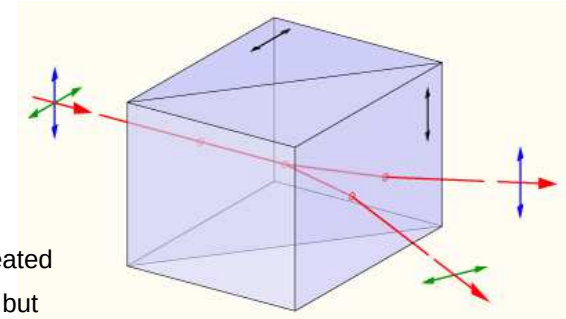

Wollaston prism

usually a crystal of calcite $CaCO_3$,

cut, turned and glued back

due to birefringence, ordinary and extra-ordinary rays are created

thanks to prism geometry these to rays are slightly divergent but start with identical phase shift

Nomarsky contrast

using additional collimation optics, the sample is illuminated by pairs of parallel rays about 0,2 μm separated.

in effect, two slightly shifted images are obtained, which are formed by cross-polarized light (to exclude interference within sample)

the second prism joins the rays which results in pseudo 3D difference image

the filter wheel equipped for various microscopy techniques (left)

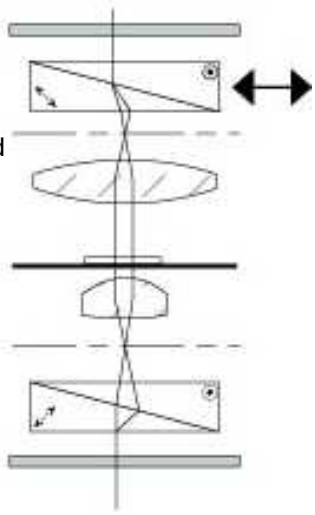

bright field image

dark field image

Nomarsky contrast

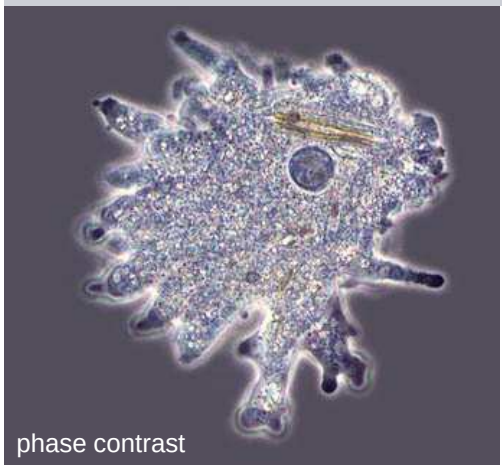

phase contrast